Actin Filament Dynamics in the Actomyosin VI Complex Is Regulated Allosterically by Calcium–Calmodulin Light Chain

ARTICLE *in* JOURNAL OF MOLECULAR BIOLOGY · SEPTEMBER 2011

Impact Factor: 4.33 · DOI: 10.1016/j.jmb.2011.08.058 · Source: PubMed

8 AUTHORS, INCLUDING:

Brannon Mccullough
University of Minnesota Twin Cities
11 PUBLICATIONS **260** CITATIONS
SEE PROFILE

Harvey F Chin
Columbia University
10 PUBLICATIONS **253** CITATIONS
SEE PROFILE

Wenxiang Cao
Yale University
34 PUBLICATIONS **806** CITATIONS
SEE PROFILE

doi:10.1016/j.jmb.2011.08.058 J. Mol. Biol. (2011) 413, 584–592

Contents lists available at www.sciencedirect.com

Journal of Molecular Biology

journal homepage: http://ees.elsevier.com.jmb

Actin Filament Dynamics in the Actomyosin VI Complex Is Regulated Allosterically by Calcium–Calmodulin Light Chain

Ewa Prochniewicz[1], Anaëlle Pierre[2,3], Brannon R. McCullough[2], Harvey F. Chin[2], Wenxiang Cao[2], Lauren P. Saunders[2], David D. Thomas[1]* and Enrique M. De La Cruz[2]*

[1]*Department of Biochemistry, Molecular Biology and Biophysics, University of Minnesota, Minneapolis, MN 55455, USA*
[2]*Department of Molecular Biophysics and Biochemistry, Yale University, New Haven, CT 06520, USA*
[3]*Département de Physique, ENS de Cachan, F-94230 Cachan, France*

Received 10 March 2011; received in revised form 5 August 2011; accepted 31 August 2011
Available online 6 September 2011

Edited by R. Craig

Keywords:
actin;
myosin VI;
calmodulin;
cooperativity;
phosphorescence spectroscopy

The contractile and enzymatic activities of myosin VI are regulated by calcium binding to associated calmodulin (CaM) light chains. We have used transient phosphorescence anisotropy to monitor the microsecond rotational dynamics of erythrosin-iodoacetamide-labeled actin with strongly bound myosin VI (MVI) and to evaluate the effect of MVI-bound CaM light chain on actin filament dynamics. MVI binding lowers the amplitude but accelerates actin filament microsecond dynamics in a Ca^{2+}- and CaM-dependent manner, as indicated from an increase in the final anisotropy and a decrease in the correlation time of transient phosphorescence anisotropy decays. MVI with bound apo-CaM or Ca^{2+}–CaM weakly affects actin filament microsecond dynamics, relative to other myosins (e.g., muscle myosin II and myosin Va). CaM dissociation from bound MVI damps filament rotational dynamics (i.e., increases the torsional rigidity), such that the perturbation is comparable to that induced by other characterized myosins. Analysis of individual actin filament shape fluctuations imaged by fluorescence microscopy reveals a correlated effect on filament bending mechanics. These data support a model in which Ca^{2+}-dependent CaM binding to the IQ domain of MVI is linked to an allosteric reorganization of the actin binding site(s), which alters the structural dynamics and the mechanical rigidity of actin filaments. Such modulation of filament dynamics may contribute to the Ca^{2+}- and CaM-dependent regulation of myosin VI motility and ATP utilization.

*Corresponding authors. E-mail addresses: ddt@ddt.biochem.umn.edu; enrique.delacruz@yale.edu.

Present address: H. F. Chin, Department of Biochemistry, Weill Cornell Medical College, New York, NY 10065, USA.

Abbreviations used: CaM, calmodulin; TPA, transient phosphorescence anisotropy; EGTA, ethylene glycol bis (β-aminoethyl ether) *N*,*N*′-tetraacetic acid; 2D, two-dimensional; ErIA, erythrosin iodoacetamide.

Introduction

Interaction of actin and myosin is required for force generation and contractility in muscle and non-muscle cells. A large body of studies on the molecular mechanism of motility approaches the problem by focusing primarily on one of the two crucial issues of this mechanism: the structure of the actomyosin interface and nucleotide-induced

0022-2836/$ - see front matter

structural changes at the light chain binding domain of myosin. However, since biochemical studies indicate functional interdependence (i.e., coupling) of the actin and light chain binding domains of several myosins, the two issues are linked, and these interrelations must be elucidated for a complete molecular understanding of myosin-based motility.

The essential light chain isoform bound to skeletal muscle myosin strongly influences actin-activated ATPase,[1] *in vitro* motility sliding velocity of actin filaments,[2] and the ability of the S1 motor domain to accelerate actin polymerization.[3] Actin-activated ATPase of smooth muscle myosin is regulated by phosphorylation-induced structural transitions in the N-terminal region of bound light chains.[4] The activity of molluscan striated muscle myosin is regulated by Ca^{2+} binding to the regulatory light chain.[5]

Light chain regulation of actin–myosin interactions requires long-range allosteric communication between the actin and light chain binding regions of myosin. Crystal structures of muscle and non-muscle myosins indicate that small movements within the myosin motor domain can be transmitted through the converter domain to the light chain binding region.[6,7] Functional interdependence between the motor properties of myosin and the light chain binding domain is particularly clear in myosin VI (herein referred to as MVI)—the only known myosin family member that moves toward the pointed end of actin filaments rather than the barbed end.[7] MVI achieves reverse directionality by rotating its lever arm in the direction opposite to that of other myosins. Such rotation is probably enabled by the presence of a unique insert between the converter and the calmodulin (CaM) light chain binding (IQ) domain, which influences coupling between the light chain binding domain orientation and the nucleotide and actin binding sites.[7,8]

The insert and IQ domains of MVI each bind a single CaM molecule. It has been suggested that the insert-bound CaM principally plays a structural role and the IQ-bound CaM may be involved in Ca^{2+}-regulation MVI function,[9] namely, slowing actin motility, actin-activated ATPase, and ADP release.[10,11] Early studies using gel densitometry showed that binding of CaM to MVI HMM dimers is not affected by Ca^{2+} up to ~100 μM.[10] Mass spectrometry confirms that CaM binding to the insert and to the IQ region is Ca^{2+} independent and that CaM binds with a higher affinity (K_d ~30 nM) to the insert domain.[9] Furthermore, structural analysis by cryo-electron microscopy shows that Ca^{2+} weakens CaM binding to the IQ domain, but not to the insert.[12] Since CaM binds the insert region of MVI independent of calcium with a high affinity,[9] while Ca^{2+} weakens the affinity of CaM for the IQ domain of MVI,[12] it is possible that CaM binding and/or a CaM-linked conformation of the IQ domain modulates actin filament stiffening.

There is increasing evidence that actin filaments adopt multiple conformational states and that the equilibria among these states are modulated by interaction with regulatory proteins, including myosin contractile proteins.[13,14] Numerous studies have shown that changes in the structural state(s) of actin modulate filament sliding and actomyosin ATPase[15,16] and that the effect of myosin on actin structure depends on the structural states of myosin.[17–19] The impact of Ca^{2+}–CaM regulation on the interaction between MVI and actin in terms of actin structural properties is less clear.

We initiated this study to determine whether Ca^{2+}–CaM regulation of MVI involves allosteric modulation of the actin binding regions that modulates the structural state fluctuations of actin. We measured the actin filament microsecond dynamics using transient phosphorescence anisotropy (TPA) and the actin filament flexural rigidity from images of thermally driven filament shape conformations acquired using fluorescence microscopy. Previously, we demonstrated that the structural dynamics of actin is an important determinant of functional properties of the actomyosin complex.[17,18,20] The present results with MVI reveal that the actomyosin interface and resulting changes in filament dynamics can be allosterically regulated by ligand-linked changes in the light chain binding domain of myosin.

Results and Discussion

Effects of MVI on actin TPA decays

MVI binding affects the TPA decays of actin filaments in a Ca^{2+}- and CaM-dependent manner (Fig. 1). In the presence of free calcium (200 μM) and no added CaM, MVI substantially increases the final anisotropy, corresponding to a reduction in the amplitude of filament microsecond rotational dynamics (i.e., torsional stiffening; Fig. 1, red), as observed with other myosin isoforms.[19] However, the effects of bound MVI are substantially diminished in the absence of calcium (i.e., with bound apo-CaM; Fig. 1, blue) or upon addition of 30 μM Ca^{2+}–CaM (Fig. 1, green). Equilibrium binding assays confirm that MVI binds actin stoichiometrically under these conditions (Fig. 2), indicating that the observed effects reflect Ca^{2+}- and CaM-dependent structural changes in actomyosin VI. Calcium and/or CaM alone has negligible effects on the TPA decays of bare actin (data not shown).

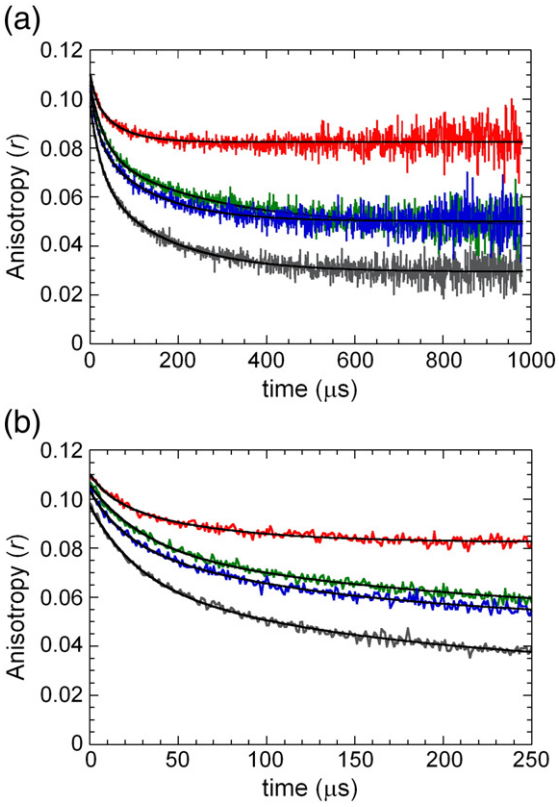

Fig. 1. Effects of Ca^{2+} and CaM on the TPA decays of actomyosin VI. Conditions: 200 μM Ca^{2+} (red), 200 μM Ca^{2+} and 30 μM CaM (green), and 1 mM EGTA (blue). Bare actin (gray) is shown for comparison. Smooth lines represent fits to the sum of two exponential terms [Eq. (1)]. Both panels show the same data over different timescales.

Ca^{2+} and CaM dependence of MVI effects on actin torsional dynamics

We evaluated the CaM dependence of actin TPA decays, specifically the final anisotropy and the average correlation time [Eqs. (1) and (2) and Fig. 3], with sub-stoichiometric MVI (myosin VI binding density = 0.25) to determine if torsional stiffening of actin filaments by MVI is regulated by CaM. The final anisotropy and the average correlation time of actin depend hyperbolically [Eq. (3)] on the [CaM] when Ca^{2+} is saturating[9,11] (Fig. 3), yielding an apparent binding affinity (K_d) of 0.6 μM (final anisotropy) to 1.5 μM (average correlation time) for Ca^{2+}–CaM binding to the IQ domain of MVI. Ca^{2+}–[CaM]-dependent changes in the individual component anisotropy amplitudes (r_1 and r_2) and correlation times (ϕ_1 and ϕ_2) yield essentially identical results as the final anisotropy and average correlation time (Fig. 4; K_d = 0.5–1.2 μM). Thus, Ca^{2+}–CaM similarly affects both slow (r_1, ϕ_1) and fast (r_2, ϕ_2) components of the anisotropy decays. We conclude, in agreement with cryo-electron microscopy

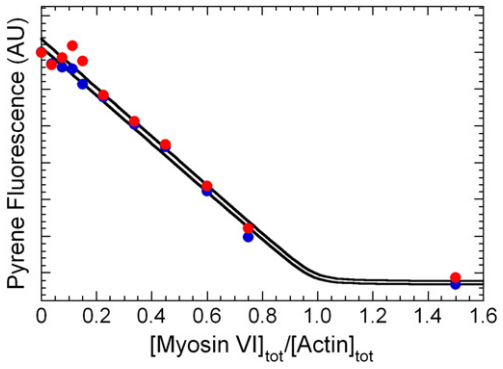

Fig. 2. Equilibrium binding of myosin VI and actin filaments. Binding of myosin VI to actin in the presence (blue) and absence (red) of 200 μM Ca^{2+} measured from pyrene actin fluorescence quenching. The continuous line is the best fit to a quadratic binding expression using the binding affinities[21] and total reactant concentrations,[22,23] yielding binding stoichiometries of 0.98 ± 0.07 and 0.98 ± 0.04 in the presence and absence of Ca^{2+}, respectively.

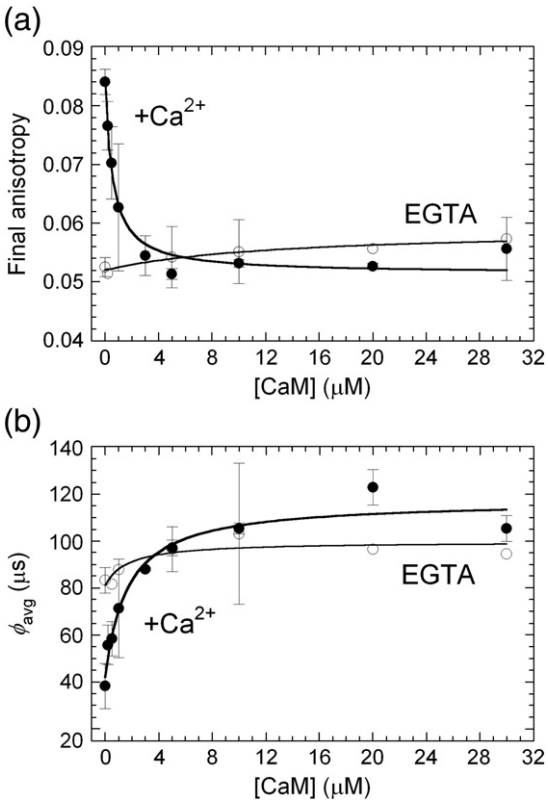

Fig. 3. Effects of exogenous CaM on TPA decays of actomyosin VI. Conditions: 200 μM Ca^{2+} (solid symbols) or 1 mM EGTA (solid symbols). The myosin binding density is 0.25. The continuous lines through the data represent the best fits to rectangular hyperbolae [Eq. (3)]. Uncertainty bars represent 1 SD from the mean.

studies,[12] that Ca^{2+} lowers the CaM binding affinity of MVI and exogenous CaM is needed to saturate the IQ domain of MVI; binding to the insert IQ peptide is much tighter ($K_d \sim 30$ nM) and independent of calcium.[9]

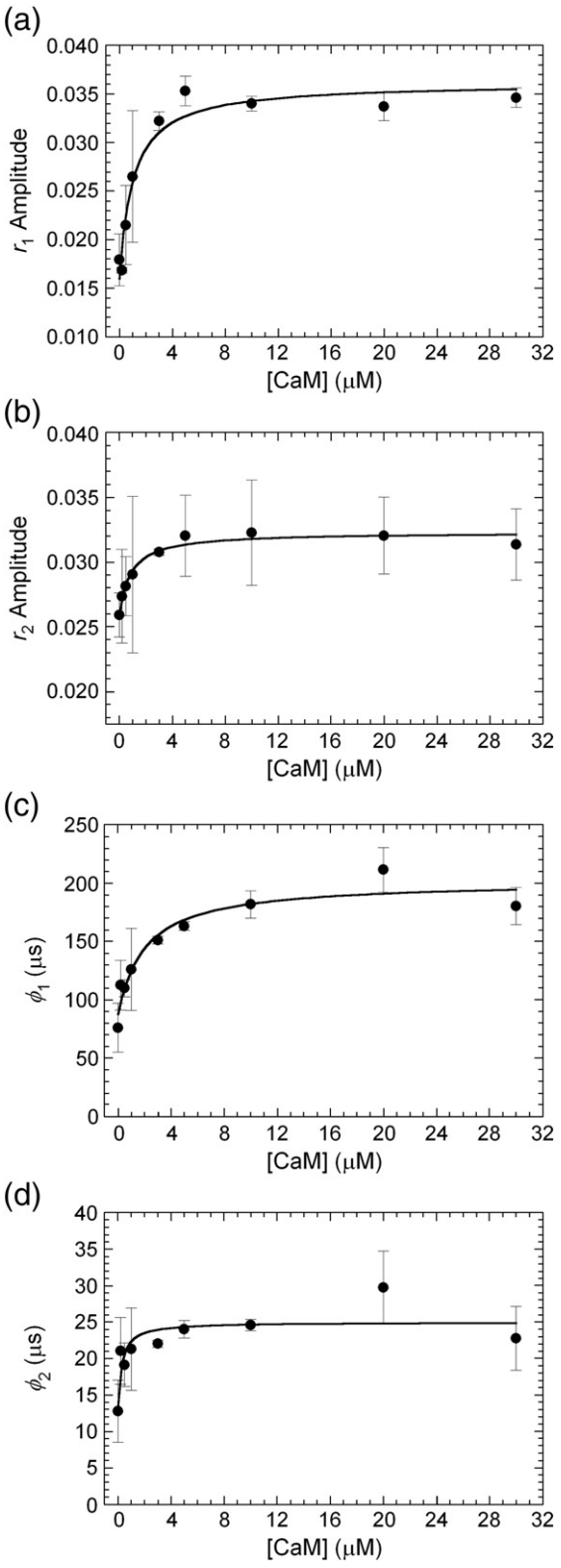

Inclusion of exogenous CaM in the absence of calcium [1 mM ethylene glycol bis(β-aminoethyl ether) *N*,*N*′-tetraacetic acid (EGTA) present] has no detectable effect on the TPA decays (Fig. 3). The simplest explanation of this result is that MVI is saturated with CaM from the initial purification and this endogenous CaM binds MVI with high affinity (K_d<130 nM) in the absence of Ca^{2+}. Thus, three distinct states that differentially affect actin rotational dynamics exist, and their distribution is dictated by the CaM and Ca^{2+} concentrations.

Allostery of MVI effects on actin torsional dynamics in the presence and absence of calcium and CaM

Experiments thus far (Figs. 1–4) evaluate the effects of CaM at a single bound MVI concentration. We have previously shown that the perturbation of actin filament microsecond torsional dynamics by various myosin isoforms displays non-nearest-neighbor (i.e., long range) cooperative interactions, such that an individual bound myosin influences the dynamics of ~10 unoccupied filament subunits.[19] For determination of whether and how the extent of filament saturation with MVI affects the regulatory effects of CaM, actin was titrated with MVI in the presence of calcium without and with CaM added at saturating (30 μM) concentration as well as in the absence of calcium, and the MVI-induced changes in the final anisotropy and average correlation time were fitted to a one-dimensional lattice model [Eq. (4) and Fig. 5]. In the presence of Ca^{2+} but absence of CaM, the increase in final anisotropy is highly cooperative, and a single bound MIV affects the dynamics of 8.5±2.7 filament subunits, similar to that observed for myosin Va.[19] A comparable cooperative unit (N=8.2±3.7) is observed in the reduction in the average correlation time.

Either addition of CaM in the presence of calcium (Ca^{2+}–CaM) or removal of calcium by EGTA (apo-CaM), two conditions favoring CaM bound at the MVI IQ domain, has substantial effects on actin dynamics. Cooperative changes in final anisotropy for Ca^{2+}–CaM and apo-CaM are less pronounced (N=4.6±0.1 and N=6.1±1, respectively), with a modest reduction in the magnitude of change in final anisotropy. The effects on the correlation time are noncooperative (Fig. 5). These data indicate that three MVI states with distinct actin filament

Fig. 4. Effects of CaM on the individual TPA decay component correlation times and anisotropy amplitudes. Conditions: 200 μM Ca^{2+}. The myosin binding density is 0.25. The continuous lines through the data represent the best fits to rectangular hyperbolae [Eq. (3)]. Uncertainty bars represent 1 SD from the mean.

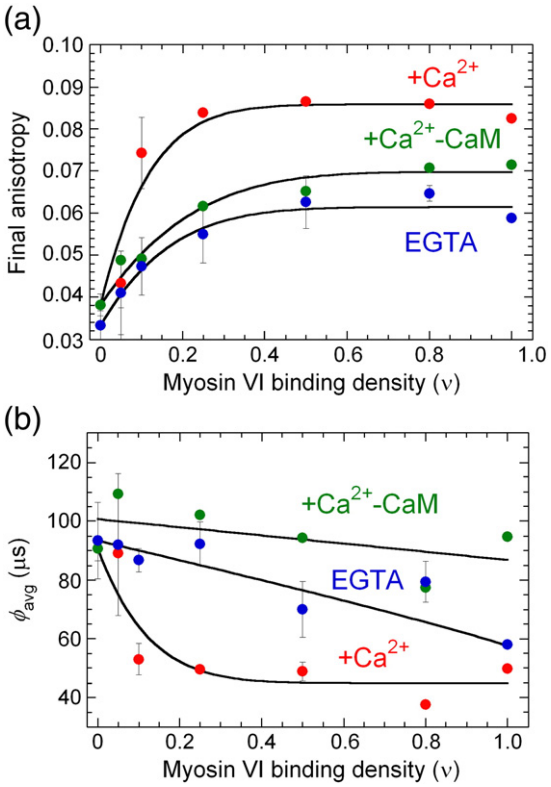

Fig. 5. Effects of myosin VI on the final anisotropy and average correlation time $\langle\phi\rangle$ of actin filaments. Conditions: 200 μM Ca^{2+} (red), 200 μM Ca^{2+} and 30 μM CaM (green), and 1 mM EGTA (blue). Myosin binding densities were calculated from the equilibrium binding affinities and total concentrations. Molar ratios ranged from 0 to 1.2 myosin per actin. The continuous lines represent the best fit of the data to the expression for binding to a linear one-dimensional lattice with cooperative non-nearest-neighbor interactions [Eq. (4)]. Uncertainty bars represent 1 SD from the mean.

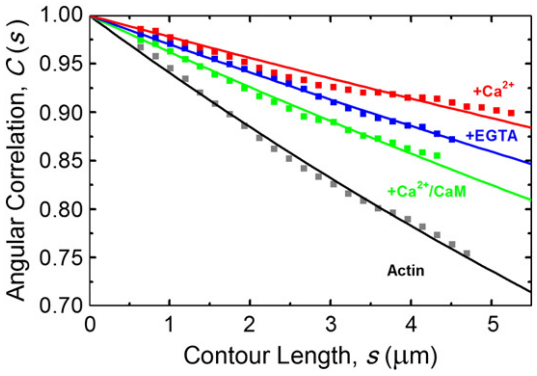

Fig. 6. Bending flexibility of actin filaments modulated by myosin VI. The best fits of the average angular correlation of actin filaments to the 2D persistence length function [Eq. (7)]: bare (black) and fully myosin VI decorated with 200 μM Ca^{2+} (red), 200 μM Ca^{2+} and 30 μM CaM (green), or 1 mM EGTA (blue) yield persistence lengths of 8.2 ± 0.2, 21.4 ± 0.7, and 12.8 ± 0.2 μm, respectively.

interactions and cooperativity (Table 1) exist in a reversible Ca^{2+}- and CaM-linked equilibrium (Table 1). MVI with bound apo-CaM or Ca^{2+}–CaM weakly affects actin filament microsecond torsional dynamics compared to other myosins (e.g., muscle myosin II and myosin Va[19]). CaM dissociation from bound MVI stiffens filaments (Fig. 6), to an extent comparable to that of other myosins.[19] Ca^{2+}- and CaM-dependent modulation of acto-MIV filament dynamics may contribute to regulation of myosin VI motility and ATP utilization.[10,11]

Bending persistence length of actomyosin VI filaments modulated by Ca^{2+} and CaM

We determined the actin and filament bending persistence length, L_p, by fitting the two-dimensional (2D) average cosine correlation function, $\langle C(s)\rangle$, to the average cosine of correlated tangential angles (θ) along segment lengths of actin filaments.[24,25] MVI increases the actin filament L_p from 8.8 ± 0.8 μm to 15 ± 1 μm (in the presence of 1 mM EGTA; Fig. 6). Adding 200 μM Ca^{2+} to actomyosin VI dissociates myosin-bound CaM and stiffens filaments, as indicated by a higher L_p of 23 ± 2 μm (Fig. 6). When additional CaM is supplemented to favor Ca^{2+}–CaM binding, actomyosin VI filaments have an L_p of 14 ± 1 μm (in the presence of 200 μM Ca^{2+} and 30 μM CaM; Fig. 6), which is comparable to actomyosin MVI in the presence of 1 mM EGTA. These measurements indicate that myosin-VI-, $Ca2^{+}$-, and CaM-dependent changes in actin

Table 1. Summary of actomyosin VI filament interactions and dynamics

Conditions	CaM occupancy	Actin cooperativity	Final anisotropy	Rotational dynamics
High Ca^{2+}, low CaM	IQ domain: unoccupied Insert: bound CaM	Induces cooperative ($N \sim 8$ subunits) actin structural changes	High	Cooperative acceleration
Ca^{2+} free (EGTA)	IQ domain: bound apo-CaM Insert: bound CaM	Weakly/noncooperative	Intermediate	Noncooperative acceleration
High Ca^{2+}, high CaM	IQ domain: bound Ca^{2+}–CaM Insert: bound CaM	Weakly/noncooperative	Intermediate	Weak acceleration

filament flexural rigidity correlate with effects on torsional dynamics assayed by TPA.

Origin of CaM-dependent actomyosin VI filament dynamics

CaM-regulated dynamics of actomyosin VI (Figs. 3 and 5) does not result from CaM binding to actin (e.g., bound CaM interaction with actin's C-terminus, as observed for the essential light chain of muscle S1[26]) since the light chain binding domain of actin-bound MVI points away from the actin filament, while that of muscle myosin II and MV tilt toward the filament.[7,8] It is more likely that CaM-regulated dynamics of MVI-bound actin occur via allosteric structural changes at the actin binding regions of MVI that originate from the light chain binding IQ domain. Reorganization of the actomyosin interface presumably compromises the energy and/or interface area between filament subunits, which influences the filament compliance.[27]

We observe a remarkable agreement between MVI-induced changes in the microsecond torsional rigidity and the millisecond flexural rigidity of actin filaments (Fig. 7). Correlated, but opposite, changes in the twisting and bending motions of actin filaments are induced by cofilin—bound cofilin lowers the torsional[28] and flexural rigidity of actin filaments.[25] These observations are consistent with a coupling between actin filament twisting and bending motions.[27] The non-nearest-neighbor effects on filament dynamics and elasticity could influence the stepping behavior of dimeric myosin VI and interaction with filament regulatory proteins.

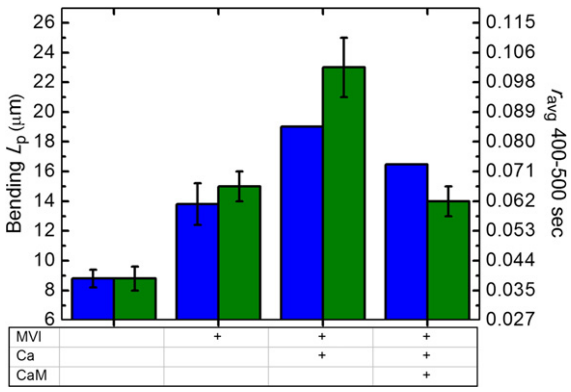

Fig. 7. CaM-dependent microsecond dynamics and millisecond flexural rigidity of actomyosin VI filaments. The amplitude of the microsecond dynamics calculated from the average anisotropy r from 400 to 500 μs (blue) and bending L_p from fits of the average angular correlation (green) of actin filaments upon the addition of saturating concentrations of myosin VI alone and with 200 μM Ca^{2+} and/or 30 μM CaM. Error bars indicate the standard error of the mean.

Actin subdomains 1 and 2 are regions likely to be affected by MVI binding as it results in reorganization of the actomyosin interface.[29] We expect MVI-induced changes in subdomain 1 to be subtle since the phosphorescence lifetime of erythrosin iodoacetamide (ErIA)-actin (156.8 ± 5.4 μs)—a sensitive indicator of accessibility of the probe environment—is not significantly affected by MVI either in the absence of Ca^{2+}–CaM (148.4 ± 3.6 μs) or in the presence of 30 μM CaM (137.1 μs). Alteration of the DNase loop within actin subdomain 2 has been implicated in determination of actin mechanical properties,[30] as well as the dynamics and distribution of structural states within actin filaments, particularly upon interaction with a variety of actin-binding proteins.[13,25,28,31–33] The increased flexibility and dynamics of cofilin-decorated actin filaments were interpreted in terms of possible disruption of stabilizing intersubunit contacts, particularly contacts involving subdomain 2 induced by rearrangement of the DNase loop.[25,33] It is possible that MVI stiffens actin filaments by stabilizing the same DNase-loop-mediated intersubunit contacts that modulate the dynamics and rigidity of actin filaments. MVI could potentially favor formation of a subset of the various actin filament subunit solution conformations.[13,14] Differences in the TPA of MVI as compared to other myosins (e.g., final anisotropy, correlation time, or cooperativity[19]) may reflect different distributions of the various filament thermal conformers that are populated with bound myosin.

Implications for biological functions of MVI

The effects of Ca^{2+}–CaM on the dynamics of actomyosin VI could potentially have functional implications. MVI stiffens actin filaments and possibly makes them more resistant to fragmentation, similar as bound MV,[19] dystrophin, and utrophin.[34] MVI is present in many non-muscle cells, and Ca^{2+}-associated modulation of actomyosin VI stiffness may be one of the structural determinants of the mechanical properties of actin bundles such as in hair cells in the inner ear.[35] Studies on the dynamics of hair bundles indicate that the bundle stiffness increases with Ca^{2+} concentration, interpreted as Ca^{2+} modulation of actin filament stiffness.[36] A significant increase in the hair bundle stiffness is observed at ~200 μM Ca^{2+},[36] which agrees with the increased actin filament stiffness upon the addition of MVI and 200 μM Ca^{2+} observed here. Thus, Ca^{2+} regulation of CaM binding to the IQ domain of MVI (i.e., by Ca^{2+} fluxes in the inner ear) likely enhances the "grip" of MVI on actin filaments and the mechanical stiffness of actin-based cytoskeletal structures.

Materials and Methods

Protein preparations

Actin was prepared from rabbit skeletal muscle and labeled with ErIA (AnaSpec)[17] or pyrene-iodoacetamide (Invitrogen) at Cys374 or Alexa 488 succinimidyl ester (Molecular Probes, Eugene, OR) and gel filtered.[25,32] A labeling efficiency with ErIA of 0.83 ± 0.13 (mean ± SD, $n = 11$) was determined from the absorbance at 538 nm using an extinction coefficient of 83,000[37] and ~0.8 for Alexa 488. Freshly prepared ErIA-labeled actin was immediately stabilized against label-induced destabilization by adding a molar equivalent of phalloidin. Actin-bound Ca^{2+} was exchanged for Mg^{2+} with 200 μM EGTA and 80 μM $MgCl_2$ immediately before polymerization. Single-headed porcine myosin VI (T406A mutant; truncated at Gly840) with bound CaM light chain[21–23] was purified from Sf9 cells by Flag affinity chromatography. The purity was >98% for all preparations. CaM was purified from *Escherichia coli* using calcium-dependent hydrophobic interaction chromatography on phenyl Sepharose 4B.[38]

TPA experiments

Phalloidin-stabilized ErIA-F-actin was diluted in KMg50 buffer [50 mM KCl, 2 mM $MgCl_2$, and 10 mM imidazole (pH 7.0) with 0.2 mM $CaCl_2$ or 1 mM EGTA] to 0.5 μM, and 0.05–0.6 μM MVI was added to form the actomyosin VI complexes, as indicated in the text. To remove residual ATP and ADP from actin, we incubated all samples prior to measurement for 20 min with 0.5 units/ml apyrase. To prolong the excited-state lifetime and prevent photo-bleaching of the dye, we removed oxygen from the sample by 5 min of incubation with glucose oxidase (55 μg/ml), catalase (36 μg/ml), and glucose (45 μg/ml).[17]

TPA data analysis: Model-independent fit to the sum of exponentials

Time-resolved phosphorescence anisotropy was measured at 25 °C as described previously[19] by recording 30 cycles of 1000 laser pulses (500 in each orientation of the polarizer). The initial anisotropy r_0, rotational correlation times ϕ_1 and ϕ_2, and corresponding amplitudes r_1 and r_2 were determined by fitting the anisotropy to the sum of two exponential terms and a constant r_∞ as described previously:[20]

$$r(t) = r_1 \exp(-t/\phi_1) + r_2 \exp(-t/\phi_2) + r_\infty \qquad (1)$$

The time course of TPA decay was fitted in the 10- to 500-μs time range. The fit quality indicated residuals <2% of the signal. Extending the fit to the full scale of decay (1 ms) increased the residuals due to lower signal-to-noise ratio at long times but yielded r_∞ values within 5% of the calculated average $r(t)$ in the 400- to 500-μs time range, since the decays are nearly completed within this timescale. The calculated average value of $r(t)$ in the 400- to 500-μs time range has been shown previously to provide the most sensitive and precise measurement of actin's microsecond rotational dynamics[20] and therefore was defined as the final anisotropy, determining the amplitude of microsecond timescale motions in actin. The component lifetimes and amplitudes of the two exponential fit were used to calculate a single weighted average correlation time $\langle\phi\rangle$:

$$\langle\phi\rangle = (\phi_1 r_1 + \phi_2 r_2) / (r_1 + r_2) \qquad (2)$$

The apparent affinity K_d of CaM to MVI was determined by fitting the effects of CaM on the final anisotropy and average correlation time (y) to a rectangular hyperbola with offset using the Origin.8 program:

$$y = y_0 + (y_{max}[\mathrm{CaM}]) / (K_d + [\mathrm{CaM}]) \qquad (3)$$

where $y_0 = y$ in the absence of CaM.

The effects of bound MVI on the observed final anisotropy (r_{obs}) of actin were analyzed in terms of the linear one-dimensional lattice model with non-nearest-neighbor interactions,[20,39] in which binding to an individual actin filament subunit allosterically affects the dynamics of a filament segment containing N protomers according to:

$$y = y_{max} - (y_{max} - y_{actin})(1-v)^N \qquad (4)$$

where y_{actin} and y_{max} are the limiting values of final anisotropy and average correlation time $\langle\phi\rangle$ at 0 and infinite concentrations of MVI, respectively, and v is the MVI binding density (i.e., bound [MVI]/[actin]). The unconstrained parameters in the least-squares fit were y_{max} and N.

The phosphorescence intensity (unpolarized) was calculated as $I(t) = (I_v(t) + 2*GI_h(t))/3$, and fitted to

$$I(t) = a_1 \exp(-t/\tau_1) + a_2 \exp(-t/\tau_2) + a_3 \exp(-t/\tau_3) \qquad (5)$$

The amplitudes (a_i) and the triplet excited-state lifetimes (τ_i) were used to calculate a single weighted average lifetime, $\langle\tau\rangle$:

$$\langle\tau\rangle = (a_1\tau_1 + a_2\tau_2 + a_3\tau_3) / (a_1 + a_2 + a_3) \qquad (6)$$

Equilibrium binding measurements

Myosin VI binding to actin filaments was measured from the [myosin] dependence of pyrene actin fluorescence quenching.[22] MVI was mixed with 500 nM phalloidin-stabilized pyrene actin and equilibrated at 25 °C (±0.1 °C) for 40–60 min in the presence of the indicated [CaM] and [Ca^{2+}]. Steady-state fluorescence intensities were measured using a Photon Technologies International (New Brunswick, NJ) Alphascan fluorescence spectrometer.

Determination of filament flexural rigidity

Cation-exchanged Alexa-488-labeled actin was polymerized in KMg50 buffer and equilibrated with and without saturating concentrations of myosin VI. Samples were diluted with KMg50 buffer supplemented with

15 mM dextrose, 100 mM DTT, 0.1 mg/ml glucose oxidase, and 20 μg/ml catalase and either 200 μM Ca^{2+}, 200 μM Ca^{2+} with 30 μM CaM, or 1 mM EGTA to a final actin concentration of 50 nM. Analysis of filaments undergoing thermal fluctuations and those adsorbed to poly-L-lysine-treated slides yielded comparable results.[24] Images of individual filaments were acquired using a Nikon Eclipse TE300 microscope equipped with a Coolsnap HQ cooled CCD camera (Roper Scientific, Tucson, AZ) and μManager, processed using imageJ† and analyzed with a code written in Matlab (The Mathworks, Natick, MA) as described previously.[25] The bending persistence length (L_p) was determined by fitting the average of >100 angular (θ) cosine correlation measurements $\langle C(s)\rangle$ of a segment length, s, corrected for measurement variance, to the following 2D correlation function:

$$\langle C(s)\rangle = \langle \cos[\theta(s) - \theta(0)]\rangle = e^{\frac{-s}{2L_p}} \quad (7)$$

Statistical analysis of data

Each result is reported as mean ± standard error of the mean, unless indicated otherwise.

Acknowledgements

Phosphorescence experiments were carried out in the Biophysical Spectroscopy Facility, University of Minnesota. The authors thank Octavian Cornea for assistance with preparation of the manuscript. This work was supported by grants from the National Institutes of Health to D.D.T. (AR32961, AG26160) and to E.M.D.L.C. (GM071688, GM071688-S1, and GM097348). E.M.D.L.C. is an American Heart Association Established Investigator (0940075N), a National Science Foundation CAREER Award recipient (MCB-0546353), and a Hellman Family Fellow. B.R.M. was supported by American Heart Association predoctoral award 09PRE2230014. H.F.C. was supported by National Institutes of Health predoctoral fellowship F31 DC009143 and in part by grants from the American Heart Association (0655849T) and Yale Institute for Nanoscience and Quantum Engineering to E.M.D.L.C.

References

1. Wagner, P. D., Slater, C. S., Pope, B. & Weeds, A. G. (1979). Studies on the actin activation of myosin subfragment-1 isoezymes and the role of myosin light chains. *Eur. J. Biochem.* **99**, 385–394.
2. Lowey, S., Waller, G. S. & Trybus, K. M. (1993). Function of skeletal muscle myosin heavy and light chain isoforms by an *in vitro* motility assay. *J. Biol. Chem.* **268**, 20414–20418.
3. Chaussepied, P. & Kasprzak, A. A. (1989). Isolation and characterization of the G-actin–myosin head complex. *Nature*, **342**, 950–953.
4. Kast, D., Espinoza-Fonseca, L. M., Yi, C. & Thomas, D. D. (2010). Phosphorylation-induced structural changes in smooth muscle myosin regulatory light chain. *Proc. Natl Acad. Sci. USA*, **107**, 8207–8212.
5. Tan, J. L., Ravid, S. & Spudich, J. A. (1992). Control of nonmuscle myosins by phosphorylation. *Annu. Rev. Biochem.* **61**, 721–759.
6. Sweeney, H. L. & Houdusse, A. (2004). The motor mechanism of myosin V: insights for muscle contraction. *Philos. Trans. R. Soc. London, Ser. B*, **359**, 1829–1841.
7. Menetrey, J., Bahloul, A., Wells, A. L., Yengo, C. M., Morris, C. A., Sweeney, H. L. & Houdusse, A. (2005). The structure of the myosin VI motor reveals the mechanism of directionality reversal. *Nature*, **435**, 779–785.
8. Wells, A. L., Lin, A. W., Chen, L. Q., Safer, D., Cain, S. M., Hasson, T. *et al.* (1999). Myosin VI is an actin-based motor that moves backwards. *Nature*, **401**, 505–508.
9. Bahloul, A., Chevreux, G., Wells, A. L., Martin, D., Nolt, J., Yang, Z. *et al.* (2004). The unique insert in myosin VI is a structural calcium–calmodulin binding site. *Proc. Natl Acad. Sci. USA*, **101**, 4787–4792.
10. Yoshimura, M., Homma, K., Saito, J., Inoue, A., Ikebe, R. & Ikebe, M. (2001). Dual regulation of mammalian myosin VI motor function. *J. Biol. Chem.* **276**, 39600–39607.
11. Morris, C. A., Wells, A. L., Yang, Z., Chen, L. Q., Baldacchino, C. V. & Sweeney, H. L. (2003). Calcium functionally uncouples the heads of myosin VI. *J. Biol. Chem.* **278**, 23324–23330.
12. Song, C. F., Sader, K., White, H., Kendrick-Jones, J. & Trinick, J. (2010). Nucleotide-dependent shape changes in the reverse direction motor, myosin VI. *Biophys. J.* **99**, 3336–3344.
13. Galkin, V. E., Orlova, A., Schroder, G. F. & Egelman, E. H. (2010). Structural polymorphism in F-actin. *Nat. Struct. Mol. Biol.* **17**, 1318–1323.
14. Kozuka, J., Yokota, H., Arai, Y., Ishii, Y. & Yanagida, T. (2006). Dynamic polymorphism of single actin molecules in the actin filament. *Nat. Chem. Biol.* **2**, 83–86.
15. Prochniewicz, E. & Yanagida, T. (1990). Inhibition of sliding movement of F-actin by crosslinking emphasizes the role of actin structure in the mechanism of motility. *J. Mol. Biol.* **216**, 761–772.
16. Kim, E., Bobkova, E., Miller, C. J., Orlova, A., Hegyi, G., Egelman, E. H. *et al.* (1998). Intrastrand cross-linked actin between Gln-41 and Cys-374. III. Inhibition of motion and force generation with myosin. *Biochemistry*, **37**, 17801–17809.
17. Prochniewicz, E., Walseth, T. F. & Thomas, D. D. (2004). Structural dynamics of actin during active interaction with myosin: different effects of weakly and strongly bound myosin heads. *Biochemistry*, **43**, 10642–10652.

† http://imagej.nih.gov/ij/

18. Prochniewicz, E., Spakowicz, D. & Thomas, D. D. (2008). Changes in actin structural transitions associated with oxidative inhibition of muscle contraction. *Biochemistry*, **47**, 11811–11817.
19. Prochniewicz, E., Chin, H. F., Henn, A., Hannemann, D. E., Olivares, A. O., Thomas, D. D. & De La Cruz, E. M. (2010). Myosin isoform determines the conformational dynamics and cooperativity of actin filaments in the strongly bound actomyosin complex. *J. Mol. Biol.* **396**, 501–509.
20. Prochniewicz, E. & Thomas, D. D. (1997). Perturbations of functional interactions with myosin induce long-range allosteric and cooperative structural changes in actin. *Biochemistry*, **36**, 12845–12853.
21. De La Cruz, E. M., Ostap, E. M. & Sweeney, H. L. (2001). Kinetic mechanism and regulation of myosin VI. *J. Biol. Chem.* **276**, 32373–32381.
22. Robblee, J. P., Olivares, A. O. & de la Cruz, E. M. (2004). Mechanism of nucleotide binding to actomyosin VI: evidence for allosteric head–head communication. *J. Biol. Chem.* **279**, 38608–38617.
23. Robblee, J. P., Cao, W., Henn, A., Hannemann, D. E. & De La Cruz, E. M. (2005). Thermodynamics of nucleotide binding to actomyosin V and VI: a positive heat capacity change accompanies strong ADP binding. *Biochemistry*, **44**, 10238–10249.
24. McCullough, B. R., Grintsevich, E. E., Chen, C. K., Kang, H., Hutchison, A. L., Henn, A. *et al.* (2011). Cofilin-linked changes in actin filament flexibility promote severing. *Biophys. J.* **101**, 151–159.
25. McCullough, B. R., Blanchoin, L., Martiel, J. L. & De la Cruz, E. M. (2008). Cofilin increases the bending flexibility of actin filaments: implications for severing and cell mechanics. *J. Mol. Biol.* **381**, 550–558.
26. Milligan, R. A., Whittaker, M. & Safer, D. (1990). Molecular structure of F-actin and location of surface binding sites. *Nature*, **348**, 217–221.
27. De La Cruz, E. M., Roland, J., McCullough, B. R., Blanchoin, L. & Martiel, J. L. (2010). Origin of twist–bend coupling in actin filaments. *Biophys. J.* **99**, 1852–1860.
28. Prochniewicz, E., Janson, N., Thomas, D. D. & De la Cruz, E. M. (2005). Cofilin increases the torsional flexibility and dynamics of actin filaments. *J. Mol. Biol.* **353**, 990–1000.
29. Volkmann, N., Ouyang, G., Trybus, K. M., DeRosier, D. J., Lowey, S. & Hanein, D. (2003). Myosin isoforms show unique conformations in the actin-bound state. *Proc. Natl Acad. Sci. USA*, **100**, 3227–3232.
30. Orlova, A. & Egelman, E. H. (1993). A conformational change in the actin subunit can change the flexibility of the actin filament. *J. Mol. Biol.* **232**, 334–341.
31. Oztug Durer, Z. A., Diraviyam, K., Sept, D., Kudryashov, D. S. & Reisler, E. (2010). F-actin structure destabilization and DNase I binding loop: fluctuations mutational cross-linking and electron microscopy analysis of loop states and effects on F-actin. *J. Mol. Biol.* **395**, 544–557.
32. De La Cruz, E. M. (2005). Cofilin binding to muscle and non-muscle actin filaments: isoform-dependent cooperative interactions. *J. Mol. Biol.* **346**, 557–564.
33. Pfaendtner, J., De La Cruz, E. M. & Voth, G. A. (2010). Actin filament remodeling by actin depolymerization factor/cofilin. *Proc. Natl Acad. Sci. USA*, **107**, 7299–7304.
34. Prochniewicz, E., Henderson, D., Ervasti, J. M. & Thomas, D. D. (2009). Dystrophin and utrophin have distinct effects on the structural dynamics of actin. *Proc. Natl Acad. Sci. USA*, **106**, 7822–7827.
35. Roux, I., Hosie, S., Johnson, S. L., Bahloul, A., Cayet, N., Nouaille, S. *et al.* (2009). Myosin VI is required for the proper maturation and function of inner hair cell ribbon synapses. *Hum. Mol. Genet.* **18**, 4615–4628.
36. Pae, S. S. & Saunders, J. C. (1994). Intra- and extracellular calcium modulates stereocilia stiffness on chick cochlear hair cells. *Proc. Natl Acad. Sci. USA*, **91**, 1153–1157.
37. Prochniewicz, E., Zhang, Q., Howard, E. C. & Thomas, D. D. (1996). Microsecond rotational dynamics of actin: spectroscopic detection and theoretical simulation. *J. Mol. Biol.* **255**, 446–457.
38. Gopalakrishna, R. & Anderson, W. B. (1982). Ca^{2+}-induced hydrophobic site on calmodulin: application for purification of calmodulin by phenyl-Sepharose affinity chromatography. *Biochem. Biophys. Res. Commun.* **104**, 830–836.
39. McGhee, J. D. & von Hippel, P. H. (1974). Theoretical aspects of DNA–protein interactions: co-operative and non-co-operative binding of large ligands to a one-dimensional homogeneous lattice. *J. Mol. Biol.* **86**, 469–489.